Published in final edited form as:
Water Res. 2016 November 01; 104: 208–219. doi:10.1016/j.watres.2016.08.006.

Investigating the Role of Biofilms in Trihalomethane Formation in Water Distirbution Systems with a Multicomponent Model

Ahmed A. Abokifa[a], **Y. Jeffrey Yang**[b], **Cynthia S. Lo**[a], **Pratim Biswas**[a,*]

[a]Department of Energy, Environmental and Chemical Engineering, Washington University in St. Louis, St. Louis, MO 63130, USA

[b]U.S. EPA, Office of Research and Development, National Risk Management Research Laboratory, Cincinnati, OH 45268, USA

Abstract

Biofilms are ubiquitous in the pipes of drinking water distribution systems (DWDSs), and recent experimental studies revealed that the chlorination of the microbial carbon associated with the biofilm contributes to the total disinfection by-products (DBPs) formation with distinct mechanisms from those formed from precursors derived from natural organic matter (NOM). A multiple species reactive-transport model was developed to explain the role of biofilms in DBPs formation by accounting for the simultaneous transport and interactions of disinfectants, organic compounds, and biomass. Using parameter values from experimental studies in the literature, the model equations were solved to predict chlorine decay and microbial regrowth dynamics in an actual DWDS, and trihalomethanes (THMs) formation in a pilot-scale distribution system simulator. The model's capability of reproducing the measured concentrations of free chlorine, suspended biomass, and (THMs) under different hydrodynamic and temperature conditions was demonstrated. The contribution of bacteria-derived precursors to the total THMs production was found to have a significant dependence on the system's hydraulics, seasonal variables, and the quality of the treated drinking water. Under system conditions that promoted fast bacterial re-growth, the transformation of non-microbial into microbial carbon DBP precursors by the biofilms showed a noticeable effect on the kinetics of THMs formation, especially when a high initial chlorine dose was applied. These conditions included elevated water temperature and high concentrations of nutrients in the influent water. The fraction of THMs formed from microbial sources was found to reach a peak of 12% of the total produced THMs under the investigated scenarios. The results demonstrated the importance of integrating bacterial regrowth dynamics in predictive DBPs formation models.

Graphical Abstract

*Corresponding author: P. Biswas (pbiswas@wustl.edu). Tel: +1-314-935-5548 Fax: +1-314-935-5464.

Supporting Information. Additional information, tables, and results as noted in the text. This material is available free of charge via the Internet at http://pubs.acs.org.

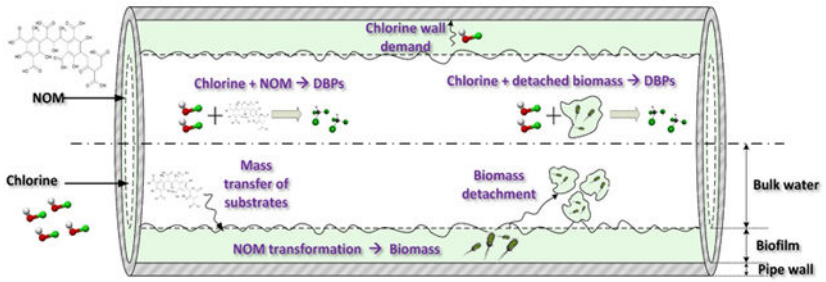

INTRODUCTION

Water quality reaching the consumer's tap is largely dictated by the physical, chemical and biological processes that take place in the distribution system. While chlorine is routinely used by drinking water utilities to inhibit microbial regrowth in their distribution systems, it reacts with the residual natural organic matter (NOM) leading to the undesired formation of carcinogenic disinfection byproducts (DBPs).[1] Moreover, the biodegradable fraction of NOM fed to the system supports the growth of biofilms[2], which plays a major role in the accumulation and release of bacterial and pathogenic species, thus compromises the microbiological quality of the treated drinking water.[3-6] Significant modeling efforts have been devoted over the past three decades to predict the formation of DBPs during water treatment [7-10]; yet more research is still required to understand their formation and transport in the distribution system. Specifically, the role of biofilms has been generally overlooked in previous modeling studies despite their ubiquitous existence in drinking water distribution systems with considerable surface biomass concentrations (up to $10^4 – 10^7$ CFU/cm^2).[11]

Previous field studies found consistently higher levels of trihalomethanes (THMs) in the distribution network and at the points of use compared to finished water.[12,13] Experimental pilot studies showed that the production of THMs in a simulated pipe environment was always higher than that observed for glass bottle tests, which was accompanied by faster chlorine consumption rates in the pipe environment.[14] This observation was attributed to the existence of a reservoir of THMs precursor material attached to the pipe wall, which can be explained by the radial mass transfer of organic compounds to the biofilm, and the bio-sorption of NOM to the extracellular polymeric substance (EPS).[15] On the other hand, biofilms were found to biodegrade haloacetic acids (HAAs), which influences their fate as their levels do not typically show a consistent increase with the residence time as in the case of THMs.[16]

The microbial carbon content associated with the biofilm has been recently shown to act as a precursor for DBPs formation in the distribution system as a result of the chlorination of both pure bacterial cells [18], or the EPS[17,19], which is largely composed of dissolved organic compounds such as polysaccharides, proteins and nucleic acids. Hence, the detachment of biomass from the biofilm matrix by either active dispersal of planktonic cells [20,21] or passive dispersal due to fluid shear or grazing [22] can contribute to the total budget of DBPs precursors. Therefore, the question arises whether this contribution is significant enough to influence the dynamics of DBPs formation in the distribution system? Moreover, what

would be the system conditions that might promote or depress this contribution? A multiple-species reactive transport model was developed to help answer these questions.

Numerous mathematical multispecies models have been developed in the literature to describe disinfectant decay and bacterial regrowth in the distribution system. [23-28] A good review of these models and their limitations can be found in the literature.[29] One of the first-generation models was presented by Lu et al. [25], which accounted for the simultaneous transport of substrates, disinfectants and microorganisms in the bulk phase and the biofilm under steady state conditions. However, their model did not account for substrate utilization and bacterial re-growth in the bulk phase, and assumed a simple first order reaction kinetics for chlorine decay. Munavalli and Kumar (2004) [23] presented a dynamic multi-component model that considered a more realistic expression for chlorine decay with a parameter that depends on the concentration of the organic carbon, while Zhang et al. (2004)[24] applied the alternating split-operator (ASO) algorithm to decouple the transport and reaction processes, which significantly simplified the numerical solution for complex reaction mechanisms of the multi-component model. Yet, all these models were mainly concerned with simulating the biological processes in the system, and none of them extended to include the formation and transport of DBPs. EPANET-MSX [30] is an advection based, public domain, generalized multi-species model that can be used to simulate the reaction and transport of any set of interacting chemical or biological species. However, like most of the other multi-species models, EPANET-MSX does not account for dispersion as a solute transport mechanism. Hence, it is not capable of providing accurate simulations for constituent transport in low flow pipes and dead-end zones. These zones are known to be responsible for most of the water quality degradation that takes place in the system due to extended residence times, and therefore require a special modeling approach such as the one we developed in our previous study (WU-DESIM).[31] With the increasing public awareness of the need for water conservation, the effect of these zones on water quality deterioration is expected to even magnify because of the generally lower flow rates.[32,33]

In this study, a 1-D multi-component reactive-transport model (WU-MSRT – Washington University Multi-Species Reactive Transport) is developed to simulate the transport and consumption of disinfectants, transformation of the biodegradable fraction of NOM into biomass through bacterial regrowth in the biofilm, the release of biomass to the bulk fluid through detachment from the biofilm, and the formation of DBPs from precursors of both microbial and non-microbial orgin. The model considers both advective and dispersive transport mechanisms, and hence is capable of efficiently simulating constituent transport under different flow conditions, ranging from the advection-dominated transport in the main trunk pipes to the dispersion-dominated transport in dead-ends. The model was applied to investigate the system conditions under which microbial carbon can significantly contribute to the overall DBPs budget in the finished drinking water including the effect of using booster re-chlorination to control bacterial regrowth in the system.

2. METHODOLOGY

2.1. Model development

2.1.1. Mathematical Model—For a water parcel moving through a distribution pipe containing disinfectants, organic compounds, nutrients, biomass and disinfection byproducts, the biochemical reactions are considered to take place at two interconnected sites within the bulk flow and in the accumulated biofilm at the pipe wall. Solute transport can be appropriately modeled by a dynamic 2-D convection-diffusion equation in cylindrical coordinates to represent the mass balance on the concentration of each of the bulk phase constituents $C_{i,b}$(x,r,t) as given by:

$$\frac{\partial \boldsymbol{C_{i,b}}}{\partial t} + \frac{\partial}{\partial x}(\bar{u}\, f(r)\boldsymbol{C_{i,b}}) - \frac{\partial}{\partial x}\left(D_{i,L}\frac{\partial \boldsymbol{C_{i,b}}}{\partial x}\right) - \frac{1}{r}\frac{\partial}{\partial r}\left(r\, D_{i,r}\frac{\partial \boldsymbol{C_{i,b}}}{\partial r}\right) = \sum_{j=1}^{N_{r,b}} r_{i,j}(\boldsymbol{C_{i=1\ldots N_{s,b}}}) \quad \text{for } 0 < r < r_f \tag{1}$$

While for wall zone constituents $C_{i,w}$, it can be written as:

$$\frac{\partial \boldsymbol{C_{i,w}}}{\partial t} - \frac{1}{r}\frac{\partial}{\partial r}\left(r\, D_{i,w}\frac{\partial \boldsymbol{C_{i,w}}}{\partial r}\right) = \sum_{k=1}^{N_{r,w}} r_{i,k}(\boldsymbol{C_{i=1\ldots N_{s,w}}}) \quad \text{for } r_f < r < r_0 \tag{2}$$

where, x & r are the axial and radial spatial coordinates, respectively (m); t is the time (sec); $\bar{u}$ is the average flow velocity in the pipe (m/sec); $f(r)$ is the radial flow distribution parameter; $D_{i,L}$ and $D_{i,r}$ are the longitudinal and radial molecular diffusivities of the solute in bulk water (m^2/sec); $D_{i,w}$ is the molecular diffusivity in the biofilm (m^2/sec); $R_{i,j}$ is the reaction involving species i in the bulk reaction j; and $R_{i,k}$ is the reaction involving species i in the wall reaction k; $N_{s,b}$ and $N_{s,w}$ are the number of species in the bulk and the wall phases; r_f is the radial location of the bulk/biofilm interface (m); and r_0 is the pipe radius (m).

In our previous study [31], the reduction of the 2-D model into a 1-D model for numerical simplicity purposes was discussed, together with the associated incorporation of the dispersive transport mechanism for the case of single-component (chlorine). The governing 1-D advection-dispersion-reaction (ADR) equation for each of the bulk phase constituents $C_{i,b}$ (x,t) can hence be written as:

$$\frac{\partial \boldsymbol{C_{i,b}}}{\partial t} + \bar{u}\frac{\partial \boldsymbol{C_{i,b}}}{\partial x} - D_i\frac{\partial^2 \boldsymbol{C_{i,b}}}{\partial x^2} = \sum_{j=1}^{N_{r,b}} r_{i,j}(\boldsymbol{C_{i=1\ldots N_{s,b}}}) - \frac{k_{f,i}}{r_h}(\boldsymbol{C_{i,b}} - \boldsymbol{C_{i,w}}) \tag{3}$$

While for wall zone constituents $C_{i,w}$ it can be written as:

$$\frac{\partial C_{i,w}}{\partial t} = \sum_{k=1}^{N_{r,w}} r_{i,k}(C_{i=1\ldots N_s,w}) + \frac{k_{f,i}}{r_h}(C_{i,b} - C_{i,w}) \quad (4)$$

where, D_l is the axial dispersion coefficient of constituent i; $k_{f,i}$ is the lumped mass transfer coefficient of constituent i at the bulk/biofilm interface (m/sec); and r_h is the hydraulic mean radius (m). Although the dynamic 2-D convection-diffusion equation provides a superior description of the solute transport compared to the 1-D model, the computational requirement for the numerical solution of a multi-species 2-D model is immense.[34] Nevertheless, previous studies showed that both models qualitatively generate similar patterns for solute concentration distributions.[34] Therefore, we applied the simplified 1-D ADR formula in this study to create WU-MSRT.

The bulk zone represents the mobile portion with both advection and hydraulic dispersion controlling the transport of bulk phase constituents in the axial direction (Eq.3). The wall zone represents a thin biofilm layer uniformly distributed over the inner pipe surface, and it represents the stagnant portion with a behavior resembling a batch reacting system with zero net convective flux (Eq.4). Constituents are assumed to have uniform concentration profiles across the pipe cross section in the bulk phase as well as within the biofilm at the wall zone. Mass transfer of constituents at the bulk/biofilm interface is modeled as a thin film concentration boundary layer (CBL) with a lumped mass transfer coefficient (k_f) as appears in the second term on the right side of (Eq.3&4). This coefficient is dependent on the flow conditions and the molecular diffusion coefficient of the component. [35-37]

The disinfectant considered in our model is chlorine, which is the most commonly adopted disinfectant by water utilities worldwide. THMs were selected as the representative DBP species for simulation because they typically constitute the largest fraction of DBPs in drinking water (typically accounts for approximately 50% of identified halogenated DBPs on a weight basis).[38] However, the developed approach in this study can be applied for simulating any other disinfectant (e.g. chloramines), or DBP species (e.g. HAAs or nitrogenous DBPs) given that the appropriate set of reaction mechanisms is implemented. Total organic carbon (TOC) was adopted as a surrogate of the NOM, while biodegradable organic carbon (BDOC) was used as a measure of the microbial growth substrate.

Monod kinetics expressions were adopted to simulate bacterial regrowth and substrate utilization in the bulk flow and within the biofilm.[23-28] The rate of biomass detachment from the biofilm is assumed to have a first order dependence on both the shear stress at the pipe wall,[35,37,39] and the attached biomass concentration. Second order reaction kinetics were used to describe chlorine-TOC reaction and THMs formation from NOM-based THMs precursors.[40-42] Details of the various processes considered in the model are included in the Supplementary material section S2.

The model consists of 10 mass balance equations (see Eq. S.1-S.10) to represent the spatial and temporal distributions of five constituents: chlorine, TOC, BDOC, biomass, and THMs,

in two phases: bulk solution (Eq. S.1- S.5), and within the biofilm at the wall (Eq. S.6- S.10) (Figure 1). To solve the complex system of partial differential equations (PDEs) that constitute the model, we applied the split-operator method (SOM) to decouple the transport and reaction processes of the multi-component system (see Supplementary material section S3).[24,43-45]

2.1.2. Modeling THMs formation from Biomass.—A simple two constituent second order kinetic model was developed to simulate the kinetics of chlorine-biomass reaction, and THMs formation from microbial carbon in the bulk solution:

$$aCl_b + bX_b \rightarrow cH_b \quad (5)$$

The reaction rate is assumed to be of second order; first order with respect to both chlorine and biomass. The formation of THMs is then proportional to the chlorine demand of the reaction, which yields the following system of differential equations representing mass balance on each of the constituents:

$$\frac{\partial Cl_b}{\partial t} = -k_{Cl,X} Cl_b X_b \quad (6)$$

$$\frac{\partial X_b}{\partial t} = -Y_X k_{Cl,X} Cl_b X_b, \qquad Y_X = \frac{b}{a} \quad (7)$$

$$\frac{\partial H_b}{\partial t} = Y_{H,2} k_{Cl,X} Cl_b X_b, \qquad Y_{H,2} = \frac{c}{a} \quad (8)$$

Where, Cl_b is the free chlorine concentration in the bulk solution (mgCl/L); X_b is the bulk biomass concentration (mgC/L); H_b is the concentration of THMs in the bulk phase (μg/L); $k_{Cl,X}$ is the second order reaction rate (L/mgC.sec); Y_X is the yield coefficient representing the consumption of chlorine reactive sites in the biomass (mgC/mgCl); $Y_{H,2}$ is the THMs formation yield as a fraction of chlorine demand (μgTHM/mgCl). The previous system of equations can be analytically solved to yield the temporal distribution of the three constituents (Clark, 1998). The model is applied to the experimental data of Wang et al. (2012b) for chloroform formation at different contact times between a bacterial cell solution and free chlorine in a bench scale reactor, where a non-linear least squares method was used to calibrate the values of $k_{Cl,X}$, Y_X and $Y_{H,2}$. The second order model yielded a good fit for the experimental measurements (Fig. 2)., and the parameter values that gave the best fit are listed in Table S3. (See Supplementary material section S4 for more discussion). A sensitivity analysis was performed on the given second order model, and the yield parameter for THM formation $Y_{H,2}$ (μgTHM/mgC) was found to have the highest influence on the

ultimate concentration of THMs, followed by the rate constant $k_{Cl,X}$ (L/mgC,sec). The yield parameter for the decay of organic carbon Y_X (mgC/mgCl) showed a conditional sensitivity, where increasing this parameter considerably lowered the THM formation, while decreasing it didn't show an effect on THM formation, which is attributed to the second order reaction being limited by the biomass concentration instead of chlorine concentration.

2.2. Model Implementation.

The model was verified by comparing the simulation results to the field measured concentrations of free chlorine and heterotrophic plate counts (HPCs) in a full-scale DWDS, and THMs in a pilot-scale pipe loop setup. The model was then used to predict THMs levels in the full-scale DWDS and to investigate the effects of hydrodynamics, water temperature, and the concentration of organics on bacterial regrowth and THMs formation from biomass in a hypothetical pipe system. Table 1 summarizes the simulations conducted in this study.

2.2.1. Bacterial dynamics module verification—The model was applied to simulate chlorine decay and bacterial regrowth in an actual DWDS, where the field measurements conducted by Prevost et al.[46] in the sampling campaign of the distribution system of the city of Laval, Quebec, Canada were used (see Table S5). The published data set included heterotrophic plate counts (HPCs) and free chlorine concentrations measured at estimated progressive residence times downstream the Pont Viau treatment plant. The sampling data reveled the seasonal dependence of organic matter concentrations, where BDOC contents were generally higher in warm water samples.[47] Data samples collected from large diameter transmission lines were used for comparison against model simulations with the exception of the final data points at a residence time of 20 hr, which were collected from small diameter pipes. The steady state conditions were simulated by running the simulations using the average flow conditions ($\overline{u} = 0.1\,\mathrm{m/s} - Re \cong 30,000$) until convergence (0.1%) was achieved for the concentrations of the ten constituents.

2.2.2. THMs module verification—The model was implemented to simulate chlorine disappearance and THMs formation in a pilot scale distribution system simulator to understand the effects of flow conditions and pipe materials. Experiments were performed on two pipe loops in the U.S. EPA's Test and Evaluation (T&E) facility in Cincinnati, Ohio, USA.[48] The first loop consisted of a new PVC pipe while the second loop was an aged ductile iron pipe with heavy scale build up. The published data set included the concentrations of THMs and free chorine in water samples collected at regular time intervals under different flow regimes including turbulent, transitional, laminar and stagnant flows. To simulate the new PVC pipe, wall zone was omitted from the model, and simulations were performed for only the five bulk-phase species.

2.2.3. Model application—The model, Wu-MSRT, was then applied to simulate a hypothetical water distribution pipe that receives the effluent of a water treatment plant with the properties tabulated in Table S4 for a total residence time of 72 hours. Re-chlorination was assumed to take place after 36 hours by introducing a chlorine dose to increase the residual concentration back to the initial level of 1 mg/L. The effects of altering the flow conditions (Re = 5000-30,000), water temperature (T = 0°C-30 °C), and initial TOC/Cl ratio

(TOC_0/Cl_0 = 1-3) on bacterial regrowth and THMs formation from biomass were investigated.

2.2.4. Parameters acquisition—The model equations comprise 22 parameters that can be categorized into three sets: i- parameters for the bacterial regrowth module; ii- parameters for the THMs formation from chlorine-NOM reaction; and iii-parameters for the THM formation from the chlorination of biomass. The values or formulae used for the three sets are given in Tables S1, S2 and S3 in the supplementary material, respectively, together with the corresponding literature sources or the actual values used to give the best fit for the verification simulations.

3. RESULTS AND DISCUSSION

3.1. Model Verification.

3.1.1. Bacterial Regrowth in the full-scale distribution system—Generally, the model showed good capability to simulate microbial regrowth and chlorine disappearance in the Pont Viau system under different temperatures and initial substrate concentrations. Fig. 3 shows the results of the model simulations plotted against field measurements for HPC and free chlorine concentrations. The model was able to demonstrate the increase in the initial rate of bacterial growth corresponding to an increase in the water temperature. In warm (T = 23.1 °C) and lukewarm (T = 13.5 °C) water samples (Figure 3a and b), rapid bacterial growth took place until reaching a maximum value corresponding to near-full substrate utilization. More importantly, the applied high chlorine dose (Cl_0 = 0.83 mg/L) for the high temperature case (T = 23.1 °C) was shown to be unable to inhibit fast microbial regrowth as shown in Figure 3a. In the cold-water samples (T = 1 °C and 1.8 °C) (Figure 3c and d), slower bacterial growth took place, where in one of the cases the chlorine dose has almost completely depleted while microbial growth is still taking place due to the remaining unmetabolized substrate (Figure 3c). Simulation results showed a noticeable sensitivity towards four of the model parameters: the maximum substrate utilization rate (u_{max}), the detachment coefficient (k_{det}), the temperature dependence rate constant (T_j), and the rate constant of the second order reaction between chlorine and bacteria ($k_{cl,x}$), which is in good agreement with previous studies.[23,45]

An interesting remark was that the same set of parameters (shown in Table S1) was used to simulate perform the four scenarios under different temperatures and initial water quality conditions. This implies that the model has a high predictive capability, where after being calibrated for a certain distribution system under different seasonal scenarios without the need for recalibration with every scenario. The only exception was for the rate of biomass detachment, which showed an obvious dependence on the temperature that could not be accounted for using a constant detachment coefficient (k_{det}) as done by previous researchers. Future experimental and modeling studies might be required to elucidate the role of temperature in biomass detachment from the biofilm.

3.1.2. THMs formation in the pilot-scale distribution system simulator—Simulations were performed for all the described experimental cases for both the DI and PVC pipe loops (except for the stagnant flow case). Comparisons with measured

concentrations were plotted in Figure 4 for the turbulent and transitional flow regimes and Figure 5 for the laminar flow regime. Overall, the model results were consistent with the measurements for both pipe loops under different hydrodynamic conditions, although it generated better results for the ductile iron pipe loop, which can be explained by the detailed consideration of the bulk and wall compartments, and properly accounting for mass transfer at the interface under different flow conditions. One important observation was that THMs formation continued in both pipe loops for several hours after complete chlorine disappearance. This illustrated the inadequacy of the second order model that implies that THMs formation should cease once chlorine is totally depleted from the system. A different model that separates the kinetics of THMs formation from chlorine decay through introducing the fast formation of a chlorinated intermediate followed by slower formation of THMs can be more suitable.[49] The model predicted minimal bacterial growth in the PVC pipe under different flow regimes due to the absence of a biofilm layer that is typically responsible for bacterial production. For the DI loop, bacterial populations showed delayed development because of the high initial chlorine concentrations, which was consistent with the experimental results as no increase in the water turbidity was noticed in the samples collected at different times. The overall THMs production from bacteria was hence negligible under these conditions.

Under laminar flow regimes (Figure 5), the model showed superior performance when compared to an advection-based technique that was simulated by ignoring the dispersive transport mechanism. Moreover, dispersive transport in real distribution network pipes will have an even higher impact on solute transport due to the dynamic nature of the inlet solute profile compared to the studied pipe loop with a fixed boundary condition. [50] To the best of the authors' knowledge, this is the first study to consider dispersive transport in modeling THMs formation in drinking water pipes. We noted that the dispersion coefficient required to fit the laminar flow regime in the DI pipe was almost one tenth of the calculated Taylor's dispersion rate, while no adjustment was required to yield a good fit for the smooth PVC pipe. This might be a result of the introduction of local mixing near the pipe wall due to the roughness of the DI pipe, which disturbs the velocity profile.

The PVC pipe loop required a slower second order reaction rate constant ($k_{cl,N}$) compared to the DI pipe loop by a factor of 28%, implying faster chlorine decay in the DI pipe, which is in agreement with the literature.[51,52] The yield coefficients for TOC decay (Y_N), and THMs formation ($Y_{H,1}$) were found to consistently increase with the initial TOC/Cl ratio (see Figure S2), which is a characteristic of the second order kinetics, and was observed by previous researchers for bench scale experiments as well. [41]

3.2. T*HMs formation in the full-scale distribution system.*

The model was applied to predict THMs levels in the Pont Viau distribution system that was used to verify the bacterial growth module. The calibrated relationships for the coefficients of THMs formation from NOM-precursors (see Figure S2), and from biomass precursors (see Table S3) were used for simulation. Since THMs formation yields are strongly dependent on the pH level, it is important to remark that the average pH of the water in the distribution system (8.1) [53] was consistent with the pH of the experimental studies used to

calibrate the model. Figure 6 shows the simulated total THM concentrations as well as the fraction of THMs formed from biomass-derived precursors. The results indicated that the THMs concentrations in the system are generally lower than the maximum permissible concentration of 80μg/L. During the earlier described sampling study, the concentration of total dissolved halogens (DOX) was sampled with the THMs levels estimated to constitute 3.8-7.9% (molar basis). [53] The provided regression model (based on field samples in the presence of free chlorine) was used herein to estimate the concentration of THMs for each one of simulated four scenarios. The calculated THMs ranges were: (a) 14.0-29.0 μg/L; (b) 9.6-20.0μg/L; (c) 4.3-8.9 μg/L; and (d) 3.9-8.1 μg/L, and they all were in good agreement with what the model predicted (Figure 6). This validated the predictive capability of the model to estimate the THMs levels in real DWDSs.

The fraction of THMs generated by biomass-derived precursors was found to depend mainly on the factors controlling the rate of bacterial regrowth, including the concentration of nutrients, water temperature, and the initial chlorination dose. The maximum fraction was observed for sample (a) (Figure 6a), which had the highest temperature (T = 23.1 °C) and initial substrate concentration ($BDOC_0$ = 0.83 mg/L) that lead to a relatively quick bacterial growth (Fig. 3a). More importantly, the use of a high dose of free chlorine (Cl_0 = 0.83 mg/L) to control the bacterial regrowth resulted in a high fraction of THMs formed from biomass-derived precursors of about 5% of the total THMs, compared to less than 2% for sample (b) that had the same nutrient concentration ($BDOC_0$ = 0.82 mg/L) but a much lower chlorine dose (Cl_0 = 0.38 mg/L). The same remark can be noted by comparing the two cold-water samples (c) and (d), with both having almost similar temperatures (T = 1 °C and 1.8 °C). More interestingly, the contribution of THMs formation was slightly higher for the cold-water sample (d) compared to the lukewarm (T = 13.5 °C) sample (b) since it had a higher chlorine dose, (Cl_0 = 0.54 mg/L), despite the higher temperature and BDOC concentration in the latter. To further elucidate the role of initial chlorine dose, we ran two more scenarios of simulation (a), with the first one having the initial chlorine concentration increased to 1.24 mg/L (1.5 times the original dose), while the other having the initial BDOC concentration decreased to 0.55 mg/L (0.66 times the original dose), to represent two alternative measures for controlling bacterial re-growth. Increasing the initial chlorine dose failed to control the fast regrowth observed in the warm sample (results not shown), but more importantly the contribution of bacteria-derived precursors increased to 7.6%. On the other hand, reducing the influent substrate concentrations was found to be more effective in controlling the fast regrowth, and the contribution dropped to 3.2%. These results highlighted the significant effect of the initial chlorine dose on the contribution of bacteria-derived precursors to THMs formation.

It is important to note that despite the generally low contribution of bacteria-derived precursors observed for the studied system, their formation mechanisms were different from that of NOM-based precursors. While THMs formation proceeds once the chlorine dose is applied, a clear delay is observed in the THMs formation from biomass until bacterial re-growth takes place. This delay period is mainly dictated by the rate of bacterial growth, which depends on the water temperature and the concentration of substrates. Furthermore, this contribution is expected to become more significant if the drinking water was re-

chlorinated [54], where bacterial re-growth would increase rapidly after the complete exhaustion of the initial chlorine dose if enough nutrients still exist in the system.

3.3. Model application – hypothetical pipe system

3.3.1. Influence of hydraulic conditions—Applying the model to the hypothetical pipe system described in Section 2.2.3 at different flow conditions, we found that the flow velocity significantly affects THMs formation from biomass as it controls bacterial regrowth through two simultaneous processes: (1) Increasing the flow velocity enhances the mass transfer of solutes across the bulk/biofilm interface. This includes the transport of disinfectants and substrates, which are the two key species controlling bacterial growth in the biofilm; (2) High shear stresses enhances the detachment of the biomass from the biofilm. The Blasius equation implemented to estimate shear stress under turbulent conditions shows that the shear stress increases with the flow velocity to a power greater than 1.

Figure 7a shows the bacterial growth dynamics in the simulated pipe system under different flow conditions. In these simulations, the flow velocity was altered to effectively change the Reynolds number. The growth scheme can be seen to have two distinct patters based on the hydraulic conditions. The first pattern takes place at Reynolds numbers in the range (5,000 – 15,000), while the second scheme takes place in the range (25,000-30,000) with a transition stage taking place in between (15,000-25,000). The first pattern is characterized by immediate bacterial growth within the first 6 h until reaching a maximum peak of HPC = 2.5-3*10^4 CFU/mL, followed by a fast mortality within the following 12 h that kills the major portion of biomass (around 70% of suspended biomass) before introducing re-chlorination after 36 h. The second growth pattern shows a delayed growth phase, where the peak biomass concentration is reached after 12h, followed by a very slow mortality rate during the following 24 h. In the first pattern, the increase in the flow velocity from Re = 5000 to 15,000 is shown to enhance the initial bacterial growth rate (higher peak concentration at an earlier time), which can be explained by the improved delivery of nutrients to the biofilm where bacterial growth mainly takes place. Although increasing the flow velocity also promotes mass transfer of chlorine to the biofilm, its overall effect on biomass mortality and inactivation is greatly reduced by the resistance factor (k_r) – (See Eq. S.(9)). Bacterial growth then reaches a maximum after fully utilizing the substrate (BDOC concentration drops to 10% of initial value in less than 4 h). However, this happens at a point where high chlorine residuals are still existent in the bulk phase (chlorine concentrations are 20% of initial dose after 6 h), which can explain the fast mortality of bacteria after reaching this maximum.

To help better understand the two patterns, the total biomass growth rate in the biofilm (Eq. S.9) can be viewed as a combination of four terms:

$$\frac{\partial X_w}{\partial t} = [substrate\,utilization - detach.\ rate - chlorination]X_w + attach.\ rate \quad (9)$$

The rate of mass transfer of bacterial cells from the bulk phase to the biofilm and the rate of natural biomass mortality have a smaller magnitude compared to the other terms and do not play a significant role in the initial growth phase, and hence were ignored in this analysis. Increasing the flow velocity will generally increase the absolute magnitudes of the three terms but with different rates. In the first pattern, the substance utilization term dominates over the detachment rate and the chlorination rate terms leading to rapid bacterial growth. A threshold is then reached somewhere at Re = 15,000-25,000, where the detachment rate combined with higher chlorine delivery becomes significant enough to initially inhibit the fast-bacterial growth in the biofilm. In the second pattern, bacterial growth slowly takes place after some delay period that increases with the flow velocity or more precisely, the shear stress as the detachment rate term increases. Since chlorine depletes by parallel reactions with NOM and pipe material demand, bacterial decay then proceeds at a much slower rate compared to the first pattern (chlorine residuals drop to only 4% of the initial dose after 10 h). When the water is re-chlorinated such that the residual concentration is raised back to the initial chlorine dose of 1 mg/L, a spontaneous death of all the remaining bacteria is observed under all simulated flow regimes. Regrowth is then inhibited after booster chlorination as the substrate has been fully utilized at this point.

The effect of flow conditions on the THMs production from biomass can be realized from Figure 7b. THMs formation from biomass can be divided into two phases; the initial-chlorination phase and the re-chlorination event. Both phases can be readily explained by the bacterial growth dynamics shown in Fig. 7a. For the initial-chlorination phase, higher THM formation rates are observed for the first growth pattern corresponding to fast bacterial growth that is concurrent with high chlorine residuals in the system. This leads the THMs yield to increase with the flow velocity until reaching the previously described threshold. For the second growth pattern, the delayed bacterial growth leads to a delay in THMs concentrations with a magnitude that corresponds to the remaining fraction of biomass in the system after the initial chlorination phase, which reflects the quantity of bacteria-derived precursors available for THMs formation. The maximum THMs yield from biomass took place at the case of Re=15,000 with the ratio of THMs formed from microbial origin of maximum 12% of the total THMs yield of the pipe (see Figure S.5a).

3.3.2. Influence of water temperature—Temperature has an interesting effect on the dynamics of bacterial regrowth where an increase in temperature affects multiple simultaneous processes: (1) a rise in the temperature leads to faster disappearance of chlorine residuals, due to the increased reaction rate with organic compounds. A simultaneous consumption of the substrate will also take place. (2) Temperature enhances bacterial growth with an exponential dependence term in the Monod's expression to a certain threshold (see Eqs. S.4 & S.9). (3) Temperature increases the reaction rate between chlorine and biomass, leading to faster mortality, and faster THMs production. Figure S3a shows the bacterial growth dynamics in the simulated pipe under different temperatures. It can be seen that as the temperature drops from 30°C to 0°C, a clear delay in the bacterial growth takes place, where the peak biomass concentration increases from 5 h for 30 °C to more than 36 h for 0 °C. This happens since for lower temperatures, substrate utilization proceeds at a slower rate, in addition to the slower chlorine consumption that leads the bulk

phase residuals to exist for a longer residence time at a higher concentration. The peak biomass concentration drops from $3*10^4$ CFU/mL to $2.2*10^4$ CFU/mL (36%) as the temperature rises 20°C to 30°C, due to the higher chlorine residual concentration at the point where the peak biomass takes place, while it drops from $3*10^4$ CFU/mL to $1*10^4$ CFU/mL (67%) as the temperature drops from 20°C to 0°C due to the consumption of the substrate. Figure S.3b illustrates the effect of temperature on THMs formation, where in the initial chlorination phase the production of THMs consistently increases with temperature from 0°C to 25°C. THMs production from the 25°C case was still larger than the 20°C case even though bacterial populations reached a higher magnitude for the latter. THMs production following the re-chlorination event was proportional to the concentration of suspended biomass in the system at the point of chlorine dosing where the maximum yield was observed for the case of 10°C. However, overall THMs production of the 25°C simulation was the highest with the fraction of THMs from bacteria-derived precursor of (−11%) (see Figure S.5b).

3.3.3 Influence of TOC/Cl ratio—Increasing the influent concentration of TOC to the system promotes bacterial growth in the distribution system as this increases the substrate concentration and simultaneously consumes chlorine residuals. Figure S4a shows the HPC concentrations in the simulated pipe under different initial TOC/Cl ratios, where the rate of microbial growth is consistently enhanced as this ratio increases. As the inlet TOC/Cl ratio increases from 1 to 3, the peak biomass concentrations increase from $1*10^4$ CFU/mL to $5*10^4$ CFU/m/L, and the time taken to reach this peak drops from 15 to 4 h. Furthermore, the surviving biomass in the system after chlorine consumption increases with the influent TOC concentration, which leads to higher THMs formation under re-chlorination condition as shown in Figure S4b. The fraction of THMs formed from bacteria-derived precursors consistently increases with the inlet TOC concentration where the maximum contribution (−10.5%) was observed for TOC/Cl=3 (see Figure S.5c).

3.4. Environmental Implications.

The results of this study demonstrated the importance of considering a parallel route for DBPs formation represented by the mass transfer of NOM to the biofilm followed by biotransformation and then detachment of biomass-derived precursors back to the bulk phase as an important alternative to the well-known DBP formation route from direct chlorination of NOM-based precursors. Previous field studies showed that a BDOC concentration of as low as 0.5 mg/L is sufficient to support bacterial regrowth if low disinfectant residuals existed in the system.[57] If water utilities responded by simply increasing the disinfectant dosage, this might lead to the adverse effect of forming excessive harmful DBPs in the distribution system, especially if the system conditions, i.e. hydraulics and temperature, assisted fast bacterial regrowth. A safer practice would be to implement a treatment technique that efficiently removes microbial substrates, such as biofilteration.[11] While HPCs are typically used as an indicator of the microbiological quality of drinking water, they are currently not enforced in the US under the safe drinking water act (SDWA), as they do not necessarily reflect a health hazard. [29,55,56] However, the current practice overlooks their important contribution to the formation of disinfection byproducts, which are potential carcinogens, teratogens or mutagens. Future modeling work on other disinfection

byproducts, such as HAAs and nitrogenous DBPs can provide the full picture on the role of biofilms in the formation and fate of the overall DBPs.

4. Conclusions

A multi species reactive transport model for simulating the transport and interactions of disinfectants, organic compounds, biomass, and disinfection byproducts (DBPs) in the pipes of drinking wate3r distribution systems was developed. This study presents the first attempt to model the formation of DBPs from organic precursors of microbial origin which is implemented to investigate the role of biofilms in the formation and fate of trihalomethanes (THMs) in the distribution system. The capability of the model to simulate chlorine decay, bacterial regrowth dynamics, and THMs formation in an actual distribution system under different hydraulic, seasonal and water quality scenarios was demonstrated.

Simulation results revealed that fast bacterial regrowth in the system increases the contribution of biomass-derived precursors to the total THMs budget, especially if high initial chlorine doses were applied to preserve the microbiological quality of the finished water. While this contribution was found to increase almost consistently with the water temperature and the concentration of nutrients, system hydraulics had a rather interesting effect, where multiple completing phenomena are significantly controlled by the flow conditions. These phenomena include the rate of mass transfer of nutrients and disinfectants from the bulk flow to the biofilm, and the rate of biomass detachment from the biofilm under shear stresses. Under the studied conditions, the contribution of bacteria-derived precursors was found to reach a maximum of 12% of the total formed THMs, which is significantly less than those formed from NOM-based precursors. However, while the formation of THMs from NOM proceeds instantly after applying the chlorine dose, the mechanism of THMs formation from bacterial sources was mainly controlled by the rates of bacterial regrowth in the system, which influenced the overall THM formation mechanism.

These results highlighted the importance of integrating bacterial growth dynamics modeling with predictive DBPs formation models. The presented model can be used by water utilities to balance the risks of microbiological vs. DBPs contamination, by simulating different scenarios for the quality of the treated drinking water effluent from the treatment plant. The model can also be implemented to identify the locations where excessive microbial regrowth or DBPs formation is expected to take place, and to further optimize the operational schemes to insure safe drinking water supply at all points in the network.

Supplementary Material

Refer to Web version on PubMed Central for supplementary material.

Acknowledgements

This work was partially funded by U.S. EPA through the CB&I Contract EP-C-4-014. The research described herein has been subjected to the Agency’s peer and administrative review and has been approved for external publication. Any opinions expressed in this paper are those of the authors and do not necessarily reflect the views of the Agency, therefore, no official endorsement should be inferred. Any mention of trade names or commercial products does not constitute endorsement or recommendation for use.

References

(1). Richardson SD; Postigo C Drinking water disinfection by-products In Emerging organic contaminants and human health; Springer Berlin Heidelberg, 2011; pp 93–137.

(2). Gagnon GA; Huck PM Removal of easily biodegradable organic compounds by drinking water biofilms: Analysis of kinetics and mass transfer. Water Res. 2001, 35 (10), 2554–2564. [PubMed: 11394791]

(3). Shen Y; Monroy GL; Derlon N; Janjaroen D; Huang C; Morgenroth E; Boppart S. a.; Ashbolt NJ; Liu W-T; Nguyen TH Role of biofilm roughness and hydrodynamic conditions in Legionella pneumophila adhesion to and detachment from simulated drinking water biofilms. Environ. Sci. Technol 2015, 49 (7), 4274–4282. [PubMed: 25699403]

(4). Shen Y; Huang C; Monroy GL; Janjaroen D; Derlon N; Lin J; Espinosa-Marzal RM; Morgenroth E; Boppart SA; Ashbolt NJ; et al. Response of simulated drinking water biofilm mechanical and structural properties to long-term disinfectant exposure. Environ. Sci. Technol 2016, 50 (4), 1779–1787. [PubMed: 26756120]

(5). LeChevallier MW; Cawthon CD; Lee RG Factors promoting survival of bacteria in chlorinated water supplies. Appl. Environ. Microbiol 1988, 54 (3), 649–654. [PubMed: 3288119]

(6). LeChevallier MW; Cawthon CD; Lee RG Inactivation of biofilm bacteria. Appl. Environ. Microbiol 1988, 54 (10), 2492–2499. [PubMed: 2849380]

(7). Brown D; Bridgeman J; West JR Predicting chlorine decay and THM formation in water supply systems. Rev. Environ. Sci. Biotechnol 2011, 10 (1), 79–99.

(8). Sadiq R; Rodriguez MJ Disinfection by-products (DBPs) in drinking water and predictive models for their occurrence: a review. Sci. Total Environ 2004, 321 (1), 21–46. [PubMed: 15050383]

(9). Ged EC; Chadik P. a; Boyer TH Predictive capability of chlorination disinfection byproducts models. J. Environ. Manage 2015, 149, 253–262. [PubMed: 25463588]

(10). Chowdhury S; Champagne P; McLellan PJ Models for predicting disinfection byproduct (DBP) formation in drinking waters: A chronological review. Sci. Total Environ 2009, 407 (14), 4189–4206. [PubMed: 19419751]

(11). Woolschlager J; Rittmann B; Piriou P Water quality decay in distribution systems – problems, causes, and new modeling tools. Urban Water J. 2005, 2 (2), 69–79.

(12). Toroz I; Uyak V Seasonal variations of trihalomethanes (THMs) in water distribution networks of Istanbul City. Desalination 2005, 176 (1), 127–141.

(13). Pieri P; Andra SS; Charisiadis P; Demetriou G; Zambakides N; Makris KC Variability of Tap Water Residual Chlorine and Microbial Counts at Spatially Resolved Points of Use. Environ. Eng. Sci 2014, 31 (4), 193–201.

(14). Rossman L. a.; Brown R. a.; Singer PC; Nuckols JR DBP formation kinetics in a simulated distribution system. Water Res. 2001, 35 (14), 3483–3489. [PubMed: 11547872]

(15). Wang Z; Hessler CM; Xue Z; Seo Y The role of extracellular polymeric substances on the sorption of natural organic matter. Water Res. 2012, 46 (4), 1052–1060. [PubMed: 22209278]

(16). Tung H-H; Xie YF Association between haloacetic acid degradation and heterotrophic bacteria in water distribution systems. Water Res. 2009, 43 (4), 971–978. [PubMed: 19070347]

(17). Wang Z; Kim J; Seo Y Influence of bacterial extracellular polymeric substances on the formation of carbonaceous and nitrogenous disinfection byproducts. Environ. Sci. Technol 2012, 46 (20), 11361–11369. [PubMed: 22958143]

(18). Wang JJ; Liu X; Ng TW; Xiao JW; Chow AT; Wong PK Disinfection byproduct formation from chlorination of pure bacterial cells and pipeline biofilms. Water Res. 2013, 47 (8), 2701–2709. [PubMed: 23499193]

(19). Wang Z; Choi O; Seo Y Relative contribution of biomolecules in bacterial extracellular polymeric substances to disinfection byproduct formation. Environ. Sci. Technol 2013, 47 (17), 9764–9773. [PubMed: 23866010]

(20). Xue Z; Sendamangalam VR; Gruden CL; Seo Y Multiple roles of extracellular polymeric substances on resistance of biofilm and detached clusters. Environ. Sci. Technol 2012, 46 (24), 13212–13219. [PubMed: 23167565]

(21). Xue Z; Seo Y Impact of chlorine disinfection on redistribution of cell clusters from biofilms. Environ. Sci. Technol 2013, 47 (3), 1365–1372. [PubMed: 23256749]

(22). Kaplan JB Biofilm Dispersal: Mechanisms, Clinical Implications, and Potential Therapeutic Uses. J. Dent. Res 2010, 89 (3), 205–218. [PubMed: 20139339]

(23). Munavalli GR; Kumar MSM Dynamic simulation of multicomponent reaction transport in water distribution systems. Water Res 2004, 38 (8), 1971–1988. [PubMed: 15087178]

(24). Zhang W; Miller CT; DiGiano F. a. Bacterial Regrowth Model for Water Distribution Systems Incorporating Alternating Split-Operator Solution Technique. J. Environ. Eng 2004, 130 (9), 932–941.

(25). Lu C; Biswas P; Clark RM Simultaneous transport of substrates, disinfectants and microorganisms in water pipes. Water Res 1995, 29 (3), 881–894.

(26). Dukan S; Yves L; Piriou P; Guyon F; Villon P Dynamic modelling of bacterial growth in drinking water networks. Water Res 1996, 30 (9), 1991–2002.

(27). Piriou P; Dukan S; Kiene L Modelling bacteriological water quality in drinking water distribution systems. Water Sci. Technol 1998, 38 (8), 299–307.

(28). Bois FY; Fahmy T; Block JC; Gatel D Dynamic modeling of bacteria in a pilot drinking-water distribution system. Water Res 1997, 31 (12), 3146–3156.

(29). Chowdhury S Heterotrophic bacteria in drinking water distribution system: A review. Environ. Monit. Assess 2012, 184 (10), 6087–6137. [PubMed: 22076103]

(30). Shang F; Uber JG; Rossman L. a. Modeling reaction and transport of multiple species in water distribution systems. Environ. Sci. Technol 2008, 42 (3), 808–814. [PubMed: 18323106]

(31). Abokifa AA; Yang YJ; Lo CS; Biswas P Water quality modeling in the dead end sections of drinking water distribution networks. Water Res 2016, 89, 107–117. [PubMed: 26641015]

(32). Rhoads WJ; Pruden A; Edwards MA Survey of green building water systems reveals elevated water age and water quality concerns. Environ. Sci. Water Res. Technol 2016, 2, 164–173.

(33). Nguyen C; Elfland C; Edwards M Impact of advanced water conservation features and new copper pipe on rapid chloramine decay and microbial regrowth. Water Res 2012, 46 (3), 611–621. [PubMed: 22153355]

(34). Naser G; Karney BW A 2-D transient multicomponent simulation model: Application to pipe wall corrosion. J. Hydro-environment Res 2007, 1 (1), 56–69.

(35). Horn H; Lackner S; Pei D; Xu J; Zhuang Q; Tse H-F; Esteban M. a. Modeling of biofilm systems: a review In Productive Biofilms; Springer, 2014; Vol. 123, pp 53–76.

(36). Rossman LA; Clark RM; Grayman WM Modeling chlorine residuals in drinking-water distribution systems. J. Environ. Eng 1994, 120 (4), 803–820.

(37). Schrottenbaum I; Uber J; Ashbolt NJ; Murray R; Janke R; Szabo J; Boccelli D Simple model of attachment and detachment of pathogens in water distribution system biofilms. In World Environmental and Water Resources Congress; 2009; Vol. 1, pp 145–157.

(38). Krasner SW; McGuire MJ; Jacangelo JG; Patania NL; Reagan KM; Aieta EM The occurrence of disinfection by-products in US drinking water. Journal-American Water Work. Assoc. 1989, 81 (8), 41–53.

(39). Horn H; Reiff H; Morgenroth E Simulation of growth and detachment in biofilm systems under defined hydrodynamic conditions. Biotechnol. Bioeng 2003, 81 (5), 607–617. [PubMed: 12514810]

(40). Clark RM Chlorine demand and TTHM formation kinetics: a second-order model. J. Environ. Eng 1998, 124 (1), 16–24.

(41). Clark RM; Sivaganesan M Predicting chlorine residuals and formation of TTHMs in drinking water. J. Environ. Eng 1998, 36, 151–165.

(42). Boccelli DL; Tryby ME; Uber JG; Summers RS A reactive species model for chlorine decay and THM formation under rechlorination conditions. Water Res 2003, 37, 2654–2666. [PubMed: 12753843]

(43). Barry DA; Miller CT; Culligan PJ; Bajracharya K Analysis of split operator methods for nonlinear and multispecies groundwater chemical transport models. Math. Comput. Simul 1997, 43 (3), 331–341.

(44). Barry DA; Bajracharya K; Crapper M; Prommer H; Cunningham CJ Comparison of split-operator methods for solving coupled chemical non-equilibrium reaction/groundwater transport models. Math. Comput. Simul 2000, 53 (1), 113–127.

(45). DiGiano FA; Zhang W Uncertainty analysis in a mechanistic model of bacterial regrowth in distribution systems. Environ. Sci. Technol 2004, 38 (22), 5925–5931. [PubMed: 15573590]

(46). Prevost M; Rompre A; Coallier J; Servais P; Laurent P; Clement B; LaFrance P; Prévost M; Rompré A; Coallier J; et al. Suspended bacterial biomass and activity in full-scale drinking water distribution systems: impact of water treatment. Water Res 1998, 32 (5), 1393–1406.

(47). Prevost M; Rompré A; Baribeau H; Coallier J; Lafrance P Service lines: their effect on microbiological quality. J. Am. Water Works Assoc 1997, 89 (7), 78–92.

(48). Yang YJ; Wre D; Impellitteri CA; Clark RM; Haught RC; Schupp DA; Panguluri S; Krishnan ER Chlorine decay and DBP formation under different flow regions in PVC and ductile iron pipes: Preliminary results on the role of flow velocity and radial mass transfer. In World Environmental and Water Resources Congress; 2008; pp 1–10.

(49). Adin A; Katzhendler J; Alkaslassy D; Rav-Acha C Trihalomethane formation in chlorinated drinking water: A kinetic model. Water Res 1991, 25 (7), 797–805.

(50). Li Z; Buchberger SG; Tzatchkov V Importance of Dispersion in Network Water Quality Modeling. In Impacts of Global Climate Change; 2005; pp 1–12.

(51). Cong L; Yang YJ; Jieze Y; Tu-qiao Z; Xinwei M; Weiyun S Second-Order Chlorine Decay and Trihalomethanes Formation in a Pilot-Scale Water Distribution Systems. Water Environ. Res 2012, 84 (8), 656–661. [PubMed: 22953450]

(52). Zhong D; Yuan Y; Ma W; Cui C; Wu Y Influences of pipe materials and hydraulic conditions on the process of trihalomethanes formation in water distribution network. Desalin. Water Treat 2012, 49 (1-3), 165–171.

(53). Baribeau H; Prevost M; Desjardins R; Lafrance P Changes in chlorine and DOX concentrations in distribution systems. J. Am. Water Works Assoc 2001, 93 (12), 102–114.

(54). Tryby ME; Boccelli DL; Koechling MT; Uber JG; Summers RS; Rossman L. a. Booster chlorination for managing disinfectant residuals. J. Am. Water Works Assoc 1999, 91 (1), 95–108.

(55). Bartram J; Cotruvo J; Exner M; Fricker C; Glasmacher A Heterotrophic plate counts and drinking-water safety: the significance of HPCs for water quality and human health.; IWA Publishing, 2003.

(56). Robertson W; Brooks T The role of HPC in managing the treatment anddistribution of drinking-water Heterotrophic Plate Counts Drink. Safety. WHOIWA Publ, pp. 233e244.

(57). DiGiano FA; Zhang W; Francisco DE; Wood M Data Collection to Support a Simplified Bacterial Regrowth Model for Distribution Systems. 2001, No. 331, 102p.

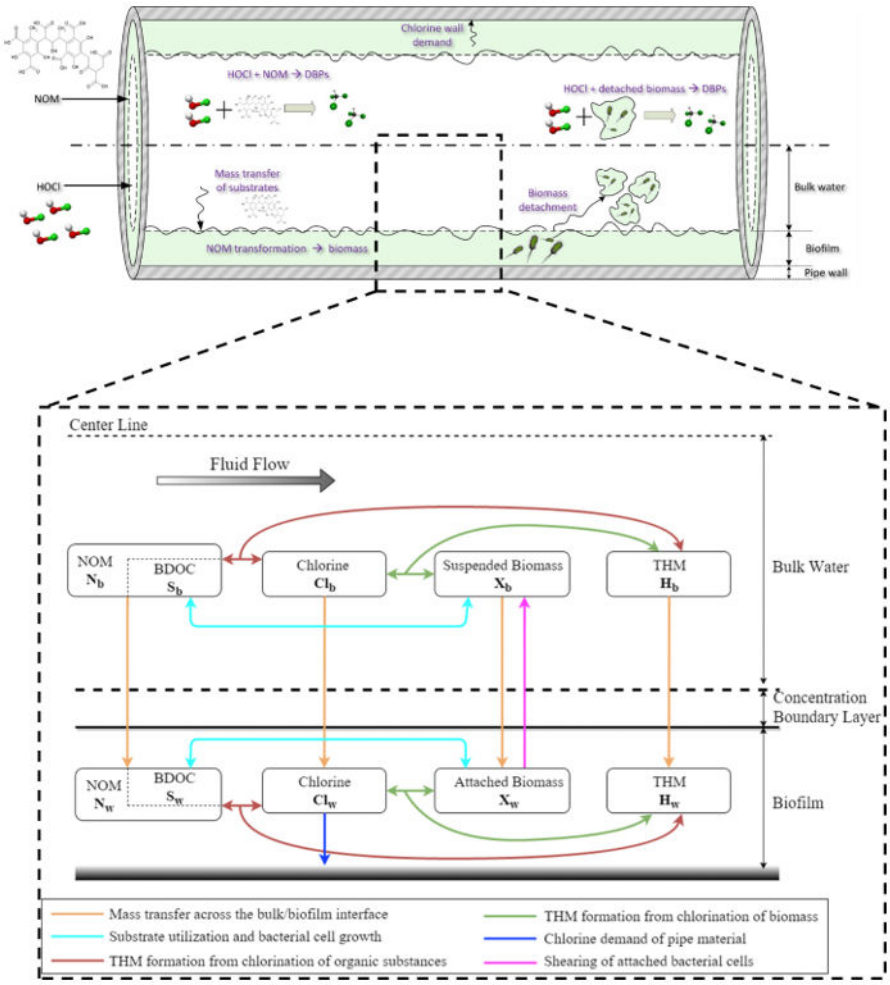

Figure 1.

Schematic diagram of the different processes considered in the model. NOM: Natural organic matter; BDOC: Biodegradable organic carbon; THM: Trihalomethanes.

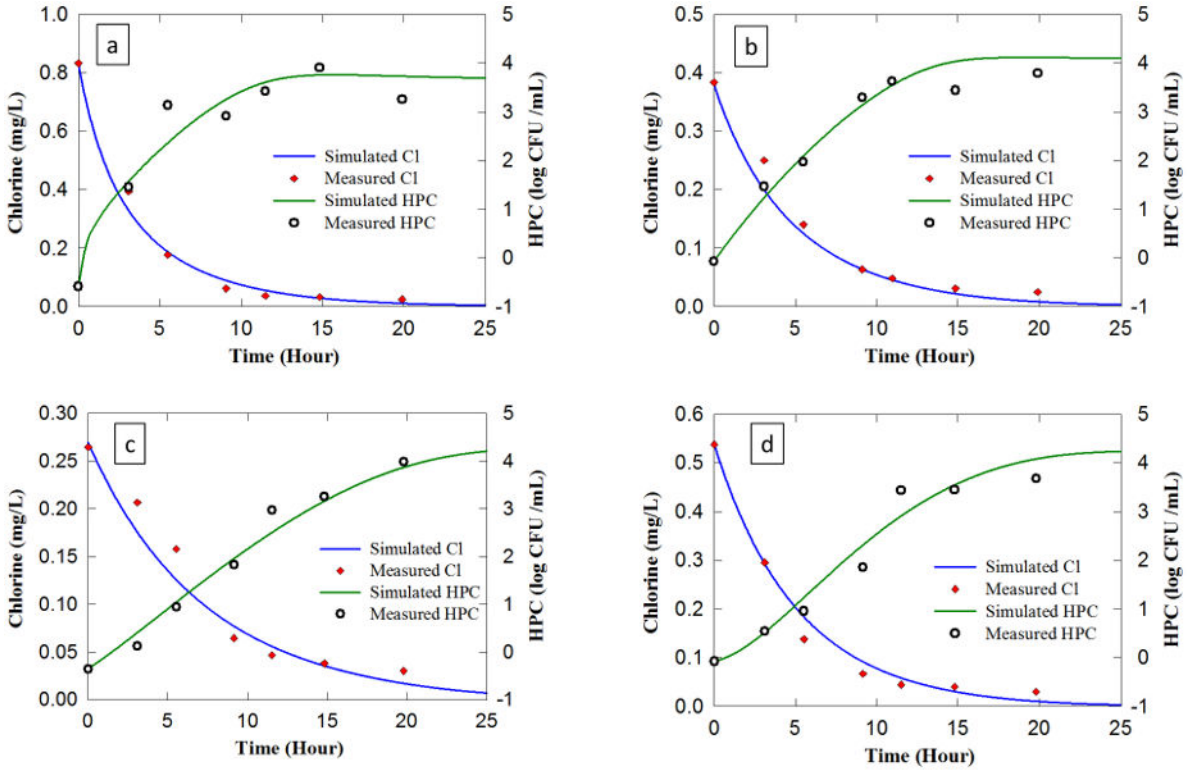

Figure 2.

Model simulation results against field measured concentrations of free chlorine (mg/l) and HPC (log CFU/ml) for Prevost et al. [46] sampling campaign: (a) 07-06-93 (T=23.1°C – $BDOC_0$ = 0.83mg/l); (b) 05-18-1993 (T=13.5°C – $BDOC_0$ = 0.82mg/l); (c) 01-12-1993 (T=1°C – $BDOC_0$ = 0.47mg/l); and (d) 12-15-1992 (T=1.8°C – $BDOC_0$ = 0.35mg/l).

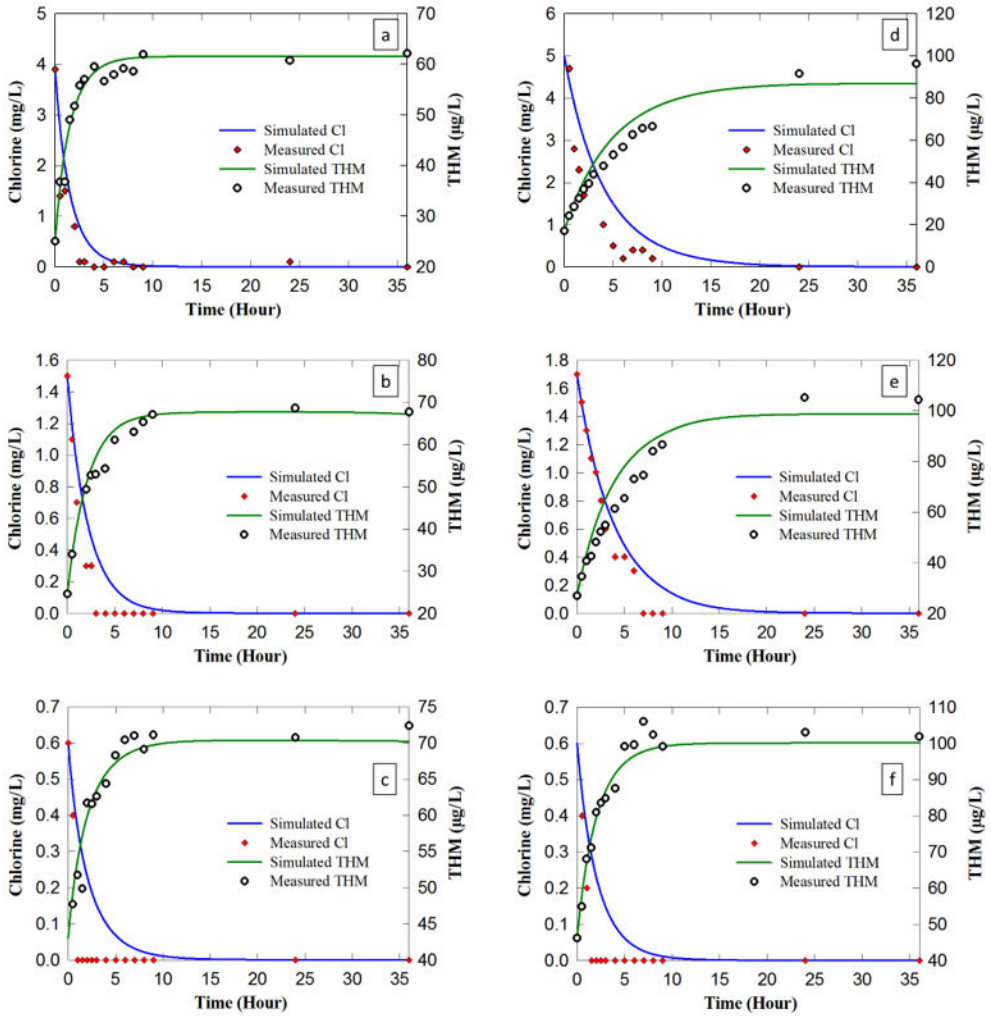

Figure 3.

Model simulation results against experimentally measured concentrations of free chlorine (mg/l) and TTHM (μg/l) for Yang et al. [48] pilot scale study – DI pipe loop: (a) Re=52,500; (b) Re=5,000 ; and (c) Re=3,500, and PVC pipe loop: (d) Re=52,500; (e) Re=5,000; and (f) Re=3,500.

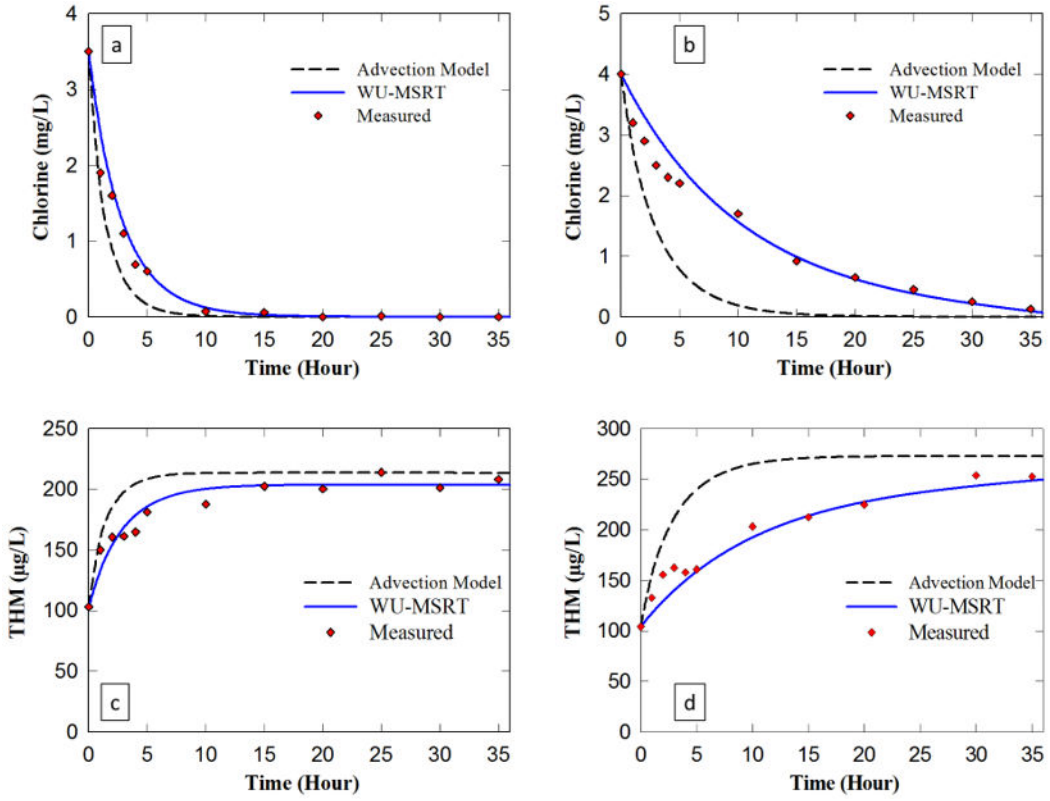

Figure 4.

Model simulation results against experimentally measured concentrations of Yang et al. [48] pilot scale study for free chlorine (mg/l) in: (a) DI pipe loop; and (b) PVC pipe loop, and TTHM (µg/l) in: (c) DI pipe loop; and (d) PVC pipe loop.

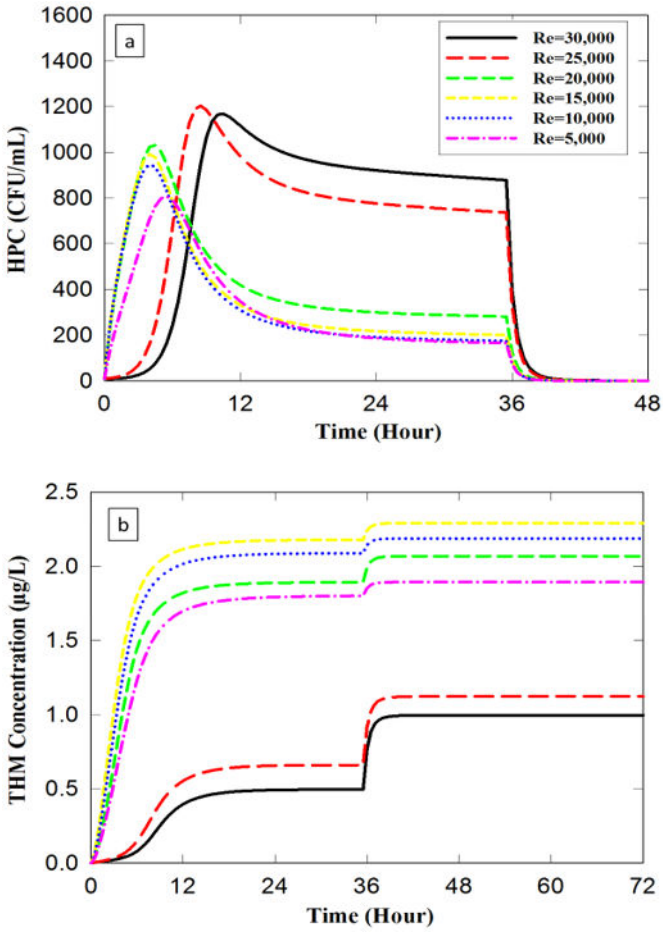

Figure 5.

Model application results for the concentrations of (a) HPC (log CFU/ml); and (b) THM (µg/l), produced from bacterial biomass precursors, under different flow conditions.

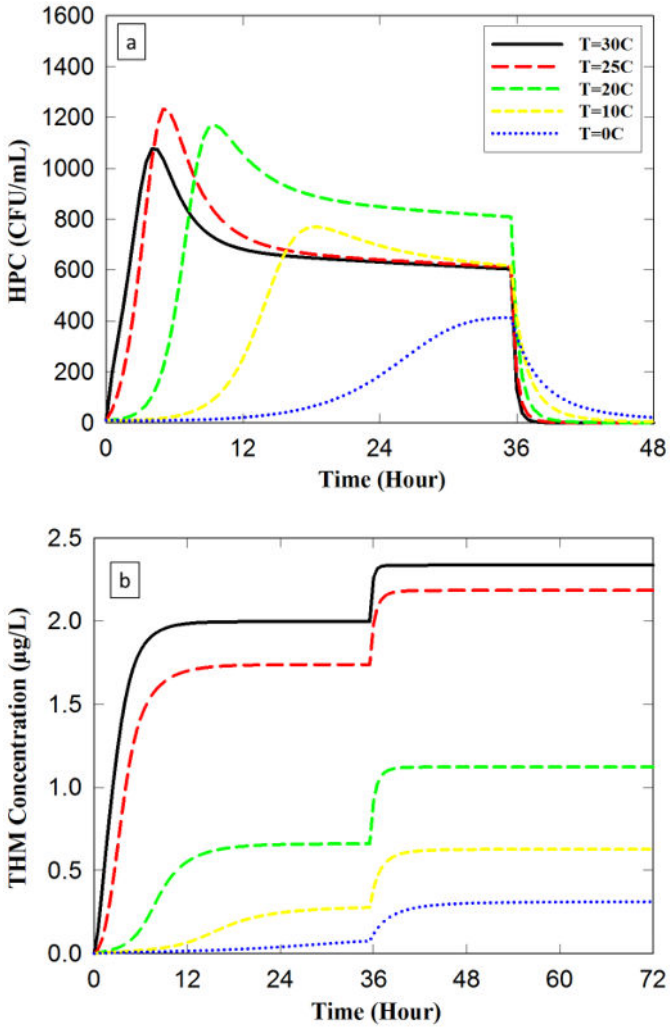

Figure 6.

Model application results for the concentrations of (a) HPC (log CFU/ml); and (b) THM (µg/l), produced from bacterial biomass precursors, under different temperature conditions.

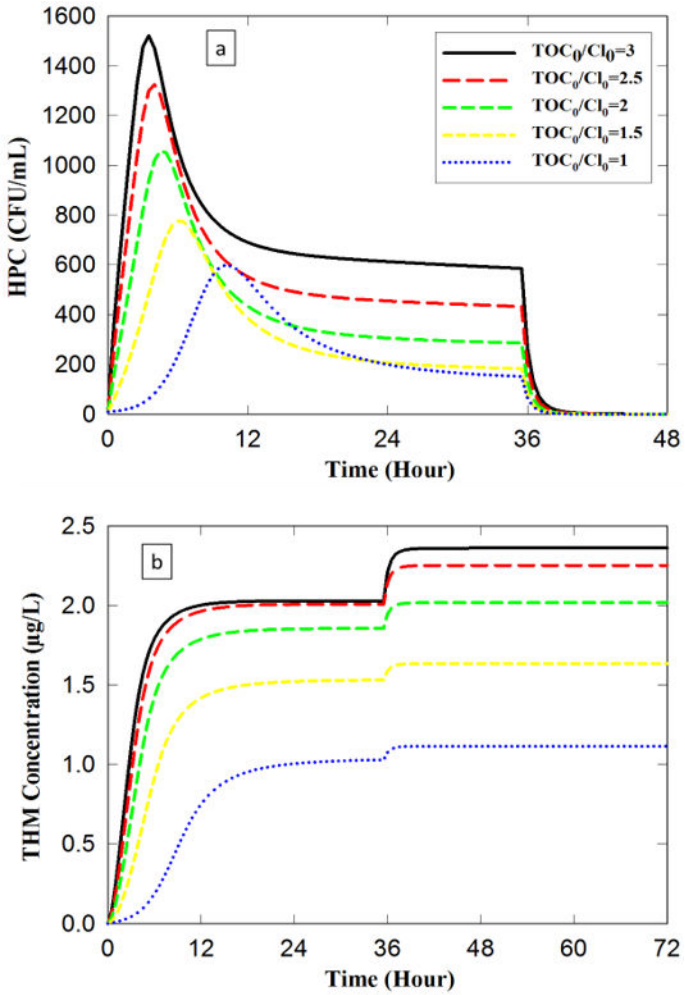

Figure 7.

Model application results for the concentrations of (a) HPC (log CFU/ml); and (b) THM (µg/l), produced from bacterial biomass precursors, under different initial TOC/Cl ratios.

Table 1.

List of simulations conducted

No.	Simulation Type	No. of Simulations	Investigated Property	Comparison Against
1	Model Verification	4	Bacterial regrowth and Chlorine decay	Field measurements - actual DWDS
2		8	THMs formation from NOM	Pilot scale pipe loop system
3	Model Application	4	Total THMs formation	Field measurements – actual DWDS
4		6		Hypothetical system - Variable Flow
5	Model Application	5	THMs formation from Biomass	Hypothetical system - Variable Temperature
6		5		Hypothetical system - Variable TOC_0